Available online at www.sciencedirect.com

ScienceDirect

International Journal of Heat and Mass Transfer 51 (2008) 1633–1645

International Journal of HEAT and MASS TRANSFER

www.elsevier.com/locate/ijhmt

Population balance model of heat transfer in gas–solid particulate systems

B.G. Lakatos [a,*], Z. Süle [b], Cs. Mihálykó [c]

[a] Department of Process Engineering, University of Pannonia, P.O. Box 158, H-8200 Veszprém, Hungary
[b] Department of Computer Science, University of Pannonia, P.O. Box 158, H-8200 Veszprém, Hungary
[c] Department of Mathematics and Computing, University of Pannonia, P.O. Box 158, H-8200 Veszprém, Hungary

Received 14 November 2006; received in revised form 10 July 2007
Available online 11 December 2007

Abstract

A population balance model is derived for heat transfer processes in gas–solid systems with intensive motion of particles in order to describe the temperature distribution of particulate phase. The model involves collisional particle–particle and particle–wall heat transfers, and continuous gas–particle, gas–wall and wall–liquid environment heat transfer processes. Collisional heat transfers are characterised by collision frequencies and random heat exchange parameters with general probability distributions with support $[0, 1]$, describing the heat transfer efficiency between the colliding solid bodies. An infinite hierarchy of moment equations, describing the time evolution of moments of the temperature of particle population is derived from the population balance equation, which can be closed at any order of moments. The properties of the model and the effects of parameters are examined by numerical experiments using the second order moment equation model of a spatially homogeneous fluidized bed.

Keywords: Population balance model; Collisional interparticle heat transfer; Collisional particle–wall heat transfer; Moment equation model; Simulation

1. Introduction

In modelling heat transfer in gas–solid processing systems, five interphase thermal processes are to be considered: gas–particle, gas–wall, particle–particle, particle–wall and wall–environment. In systems with intensive motion of particles, the particle–particle and particle–wall heat transfers occur through interparticle and particle–wall collisions so that both experimental and modelling study of these collisional processes is of primary interest.

Particle–particle and particle–wall heat transfers may result from three mechanisms: heat transfers by radiation, heat conduction through the contact points between the collided bodies, and heat transfers through the gas lens at the interfaces between the particles, as well as between the wall and particles collided with that. The first mechanism seems to be negligible below temperature 600 °C and will not be considered here. Heat conduction through the contact points was modelled by Schlünder [1], Martin [2] and Sun and Chen [3] developing analytical expressions for particle–particle and particle–wall contacts. Often, however, the conductive heat exchange can hardly be isolated from the third mechanism occurring through the gas lens at the interfaces of the colliding bodies. Based on this mechanism, Delvosalle and Vanderschuren [4,5] developed a deterministic model for describing particle–particle heat transfer, while a model for heat transfer through the gas lens between a surface and particles was derived by Molerus [6]. Blickle et al. [7] and Mihálykó et al. [8], based on the assumption that most factors characterising the simultaneous heat transfer through the contact point and the gas lens are stochastic quantities described the collisional interparticle heat transfer by means of an aggregative random parameter.

* Corresponding author. Tel.: +36 88 624 210; fax: +36 88 624 171.
E-mail address: lakatos@fmt.uni-pannon.hu (B.G. Lakatos).

0017-9310/$ - see front matter © 2007 Elsevier Ltd. All rights reserved.
doi:10.1016/j.ijheatmasstransfer.2007.07.014

Nomenclature

a	surface area, m^2
Ar	Archimedes number ($Ar = g\rho_g d_p^3(\rho_p - \rho_g)/\mu_g^2$)
b	conversion density function
B	conversion distribution function
c	specific heat, J kg^{-1} K^{-1}
D	diameter of the bed, m
D_l	diameter of the cooling jacket, m
f	density function
F	distribution function
g	acceleration of gravity, m s^{-2}
G	growth rate of particle temperature, K s^{-1}
h	heat transfer coefficient, W m^{-2} K^{-1}
K_{pg}	rate coefficient of temperature, s^{-1} ($K_{pg} = h_{pg}a_{pg}/(m_p c_p)$)
k	thermal conductivity, W m^{-1} K^{-1}
m	mass, kg
M_k	kth order moment of particle temperature
m_k	normalised kth order moment of particle temperature
N	number of particles
n	population density function, no. m^{-3} K^{-1}
N	population distribution function, no. m^{-3}
Nu_g	Nusselt number for gas ($=h_{gw}D/k_g$)
Nu_l	Nusselt number for liquid ($=h_{lw}D/k_l$)
$\boldsymbol{O}$	order of magnitude
p_j	weight parameter ($=m_k c_k/(m_j c_j + m_k c_k)$)
p_k	weight parameter ($=m_j c_j/(m_j c_j + m_k c_k)$)
Pr_g	Prandtl number for gas ($=\mu_g c_g/k_g$)
Pr_l	Prandtl number for liquid ($=\mu_l c_l/k_l$)
Q	heat, J
q	volumetric flow rate, m^3 s^{-1}
r	source function
Re_g	Reynolds number for gas ($=\rho_g u_g D/\mu_g$)
Re_l	Reynolds number for liquid ($=\rho_l u_l(D_l - D)/\mu_l$)
Re_p	Reynolds number for particle ($=\rho_g u_g d_p/\mu_g$)
S	activity function, frequency of collisions
T	temperature, K
t	time, s
u	superficial velocity, m s^{-1}
V	volume, m^3
$\boldsymbol{x}$	vector of space variables
y	variable
z	variable
$\mathbf{1}$	Heaviside function
$\langle .,. \rangle$	scalar product of functions

Greek symbols

θ	contact time, s
$\boldsymbol{\theta}$	vector of random parameters
β	beta function
ρ	density, kg m^{-3}
δ	Dirac-delta function
κ	parameter
ω	random parameter of heat transfer
φ	smooth function of compact support
μ	viscosity, Pa s
ε	void fraction of the bed
ϕ	weight parameter ($0 \leqslant \phi \leqslant 1$)
σ^2	variance of particle temperature

Subscripts and superscripts

ω	random parameter
g	gas
in	input
l	liquid
max	maximal value
mf	incipient velocity of fluidization
min	minimal value
p	particle
pg	particle–gas
pp	particle–particle
pw	particle–wall
t	entrainment velocity of fluidization
w	wall
wg	wall–gas
wl	wall–liquid

Various models have been used for making possible of computing the effects of collisional heat transfer processes in gas–solid systems with intensive motion of particles. Li and Mason [9], simulating non-isothermal gas–solid two-phase flow in pneumatic transport pipes by a distinct element method (DEM) included both the particle–particle and particle–wall heat transfer processes. Lathouwers and Bellan [10] modelled the thermofluid dynamics of dense gas–solid reactive mixtures in fluidised beds using a multi-fluid approach and taking into consideration also the effects of particle–particle heat transfer. Mansoori et al. [11] modelled an upward vertical turbulent gas–solid duct flow including the collisional particle–particle heat transfer into a four-way interaction Eulerian–Lagrangian computational scheme. An age distribution model was applied by Burgschweiger and Tsotas [12] for describing particle–particle heat transfer in modelling gas fluidised bed drying. Zhou et al. [13] used the discrete element method-large eddy simulation (DEM-LES) to model coal combustion in a bubbling fluidised bed computing also colliding particle–particle heat transfer. Mihálykó et al. [14], using a stochastic approach derived a population balance model for heat transfer in gas–solid systems taking into account the particle–particle heat transfer. Mansoori et al. [15] included both the collisional particle–particle and particle–wall heat transfer events into the four-way interaction Eulerian–Lagrangian model of gas–solid turbulent flow in a riser. Chagras et al. [16] modelled turbulent gas–solid flows in heated pipes using an Eulerian–Lagrangian approach considering collisional heat transfer by conduction and handling interparticle collisions by means of a probabilistic model. Lakatos et al. [17,18] and Süle et al. [19] extended the population balance model for spatially distributed systems, coupling the population balance equation of particles with axial dispersion and compartmental models of particle flow.

Most of the works modelling explicitly heat transfer processes by collisions handled also the particle–wall heat transfer by deterministic models, using the analytical expressions of Sun and Chen [3] and Molerus [6]. The particle–wall contact characteristics, such as contact time, contact angle and contact distance, as it was shown by Sommerfeld [20,21] studying a turbulent two-phase flow in a vertical channel by experiments and simulation, and demonstrated by Hamidipour et al. [22] experimentally applying radioactive particle tracking in a gas–solid fluidised bed are, in principle, of probabilistic nature. Therefore, the random parameter heat transfer model [14,18] can also be applied for describing heat exchange by particle–wall collisional interactions, formulating in this way a comprehensive population balance model for heat transfer processes in non-isothermal gas–solid systems characterised by intensive motion of particles.

In the present paper, the population balance model is extended to describe also wall–particle heat transfer processes by collisions, taking into account the gas–solid, wall–gas and wall–environment heat transfers as well. The modelling problem of a continuously operated gas–solid system is considered in which both the gas and solid phases are assumed to be well mixed. Using this approach, a population balance model is developed for describing the variation of the temperature distribution of particles, and of the gas, wall and environment temperatures. An infinite hierarchy of moment equations is derived, and a second order moment equation model is applied to investigate the properties of the model and to analyze the system heat transfer processes by simulation.

2. Particle–particle and particle–wall heat transfer: population balance equations

Consider a continuous gas–solid system into which particles of different temperatures are fed with constant volumetric flow rate q_p, while the gas of given temperature flows in with volumetric flow rate q_g, as it is shown schematically in Fig. 1. Heat exchange occurs between the gas, particles and the wall, as well as between the processing system and the environment through the wall where the environment is represented by a continuously flowing finite capacity liquid medium. Since we are interested only in heat transfer phenomena we assume no mass transfer pro-

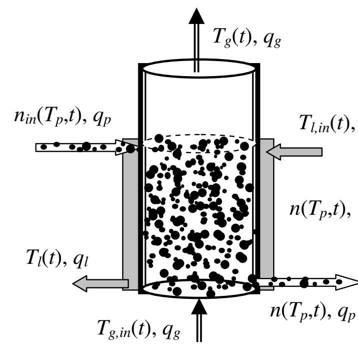

Fig. 1. Schematic diagram of a jacketed gas–solid fluidized bed.

cesses as it usually takes place in particulate energy conversion systems.

Let us assume that the particles, because of mechanical or hydraulic mixing of the suspension are in intensive motion in the gas phase so that the particle–particle and particle–wall heat transfers occur only by collisions. Therefore, this is a typical disperse system with interactive population of particles so that we can apply directly the modelling approach presented by Lakatos et al. [17,18].

Additional assumptions concerning the system are as follows.

(1) The particles are of constant size and are not changed during the process.
(2) The temperature inside a particle is homogeneous.
(3) The system is operated under steady state hydrodynamic conditions, and the influence of thermal changes on the hydrodynamics is negligible.
(4) The heat transfer between the gas and particles, wall and gas, as well as the wall and environment are continuous processes.
(5) There is no heat source inside the particles.
(6) The heat transfer by radiation is negligible.
Under such assumptions, the state of a particle is formed by four external variables, the space coordinates and time, and a single internal variable being the particle temperature. However, now we focus our attention on developing the population balance model describing the heat transfer processes so that we assume:
(7) Both the gas and particle phases, as well as the environmental cooling or heating medium are perfectly mixed.

A perfectly mixed vessel represents a spatially zero-dimensional system therefore the state of a particle $(\boldsymbol{x}, T_p, t)$, reduces to the pair of variables (T_p, t). As a consequence, the state of the particle population is given by the population density function $n(T_p, t)$ which, in principle, describes the temperature distribution of particles and the expression $n(T_p, t)\mathrm{d}T_p$ provides the number of particles in a unit volume of system having temperature in the interval $(T_p, T_p + \mathrm{d}T_p)$ at time t.

Under such conditions, as it shown schematically in Fig. 2, particles participate in gas–solid heat transfer, that is a continuous local process, and simultaneously take part in two non-local, non-continuous elementary heat exchange processes: the first one occurs between the elements of the same particle population, while the second process occurs between the elements of two different populations: the population of particles and the wall, being in this case a degenerate single element population. Therefore the population density function of the wall is given by the Dirac-delta function $n_{\mathrm{w}}(T,t)=\delta(T-T_{\mathrm{w}}(t))$ where $T_{\mathrm{w}}(t)$ denotes the wall temperature at moment of time t. As a consequence the population balance equation governing the population density function of particles, derived as a special case of the general form [18] is written as

$$
\begin{aligned}
V\frac{\partial n(T_{\mathrm{p}},t)}{\partial t} &= -V\frac{\partial}{\partial T_{\mathrm{p}}}\left(G_T^{\mathrm{pg}} n(T_{\mathrm{p}},t)\right) \\
&\quad - V\int_{\Omega_{\mathrm{pp}}}\frac{1}{N(t)}\int_{T_{\mathrm{p,min}}}^{T_{\mathrm{p,max}}}\int_{T_{\mathrm{p,min}}}^{T_{\mathrm{p,max}}} S_{\mathrm{pp}}(T_{\mathrm{p}}|z)b_{\mathrm{pp}}(T_{\mathrm{p}},y|z,\omega_{\mathrm{pp}}) \\
&\quad \times n(T_{\mathrm{p}},t)n(z,t)\,\mathrm{d}z\,\mathrm{d}yF_{\omega_{\mathrm{pp}}}(\mathrm{d}\omega_{\mathrm{pp}}) \\
&\quad + V\int_{\Omega_{\mathrm{pp}}}\frac{1}{N(t)}\int_{T_{\mathrm{p,min}}}^{T_{\mathrm{p,max}}}\int_{T_{\mathrm{p,min}}}^{T_{\mathrm{p,max}}} S_{\mathrm{pp}}(y|z)b_{\mathrm{pp}}(y,T_{\mathrm{p}}|z,\omega_{\mathrm{pp}}) \\
&\quad \times n(y,t)n(z,t)\,\mathrm{d}y\,\mathrm{d}zF_{\omega_{\mathrm{pp}}}(\mathrm{d}\omega_{\mathrm{pp}}) \\
&\quad - V\int_{\Omega_{\mathrm{pw}}}\int_{T_{\mathrm{p,min}}}^{T_{\mathrm{p,max}}}\int_{T_{\mathrm{w,min}}}^{T_{\mathrm{w,max}}} S_{\mathrm{pw}}(T_{\mathrm{p}}|z)b_{\mathrm{pw}}(T_{\mathrm{p}},y|z,\omega_{\mathrm{pw}}) \\
&\quad \times n(T_{\mathrm{p}},t)n_{\mathrm{w}}(z,t)\,\mathrm{d}z\,\mathrm{d}yF_{\omega_{\mathrm{pw}}}(\mathrm{d}\omega_{\mathrm{pw}}) \\
&\quad + V\int_{\Omega_{\mathrm{pw}}}\int_{T_{\mathrm{w,min}}}^{T_{\mathrm{w,max}}}\int_{T_{\mathrm{p,min}}}^{T_{\mathrm{p,max}}} S_{\mathrm{pw}}(y|z)b_{\mathrm{pw}}(y,T_{\mathrm{p}}|z,\omega_{\mathrm{pw}}) \\
&\quad \times n(y,t)n_{\mathrm{w}}(z,t)\,\mathrm{d}y\,\mathrm{d}zF_{\omega_{\mathrm{pw}}}(\mathrm{d}\omega_{\mathrm{pw}}) \\
&\quad + V\int_{\Theta}\frac{1}{N(t)}\int_{T_{\mathrm{p,min}}}^{T_{\mathrm{p,max}}} r(T_{\mathrm{p}},t|z,\boldsymbol{\theta})n(z,t)\,\mathrm{d}zF_{\boldsymbol{\theta}}(\mathrm{d}\boldsymbol{\theta},t)
\end{aligned} \tag{1}
$$

where

$$N(t)=\int_{T_{\mathrm{p,min}}}^{T_{\mathrm{p,max}}} n(T_{\mathrm{p}},t)\,\mathrm{d}T_{\mathrm{p}}, \tag{2}$$

V is the volume of the system, and θ denotes some vector of random variables characterising the possible random effects on the source term of particles.

The first term on the right hand side of Eq. (1) describes the variation of the population density function $n(T_{\mathrm{p}},t)$ due to gas–solid heat transfer where

$$
\begin{aligned}
G_T^{\mathrm{pg}} &= \frac{\mathrm{d}T_{\mathrm{p}}(t)}{\mathrm{d}t} = \frac{h_{\mathrm{pg}}a_{\mathrm{pg}}}{m_{\mathrm{p}}c_{\mathrm{p}}}(T_{\mathrm{g}}(t)-T_{\mathrm{p}}(t)) \\
&= K_{\mathrm{pg}}(T_{\mathrm{g}}(t)-T_{\mathrm{p}}(t))
\end{aligned} \tag{3}
$$

is the rate equation of the temperature of a particle of mass m_{p} immersed in the gas of temperature T_{g}.

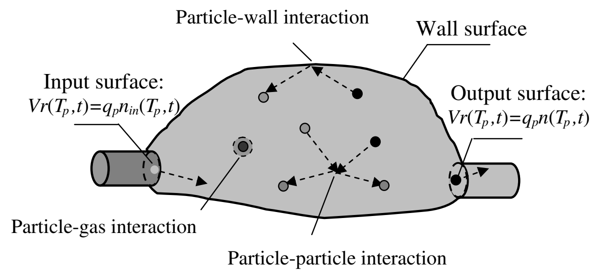

Fig. 2. Schematics of interactions of particle population in a continuous gas–solid system with intensive motion of particles.

The second and third terms on the right hand side of Eq. (1) represent non-local changes of the population density function due to interparticle collisions, while the third and fourth terms describe the variation of $n(T_{\mathrm{p}},t)$ as a result of collisions of particles with the wall. Here, two different pairs of functions express the intensities of interactions of particles with other particles and the wall, respectively. $S_{\mathrm{pp}}(T_{\mathrm{p}}|z)$ denotes the activity function characterising the intensity of collision interactions between the particles inducing discontinuous temperature changes inside the particles, while $b_{\mathrm{pp}}(y,T_{\mathrm{p}}|z,\omega_{\mathrm{pp}})$ is the conversion density function describing the results of these events, i.e. $b_{\mathrm{pp}}(y,T_{\mathrm{p}}|z,\omega_{\mathrm{pp}})\mathrm{d}T_{\mathrm{p}}$ expresses the fraction of particles that become of temperature $(T_{\mathrm{p}},T_{\mathrm{p}}+\mathrm{d}T_{\mathrm{p}})$ as a result of collisional heat transfer interactions of particles of temperature y collided with particles of temperature z in a heat transfer process characterised with random parameter ω_{pp}. The activity and conversion density functions $S_{\mathrm{pw}}(T_{\mathrm{p}}|z)$ and $b_{\mathrm{pw}}(y,T_{\mathrm{p}}|z,\omega_{\mathrm{pw}})$ have similar interpretations for particles with respect to particle–wall collisional heat transfer interactions where now z denotes the wall temperature. In this case, the result of a particle–wall heat transfer event is characterised by the random variable ω_{pw}.

In the present system, the feed and withdrawal rates of particles are the only source and sink terms which can be written as $Vr(T_{\mathrm{p}},t|z,\theta)=q_{\mathrm{p}}(t)n_{\mathrm{in}}(T_{\mathrm{p}},t)-q_{\mathrm{p}}(t)n(T_{\mathrm{p}},t)$ so that the last term on the right hand side of Eq. (1) takes the form

$$
\begin{aligned}
&V\int_{\Theta}\frac{1}{N(t)}\int_{T_{\mathrm{p,min}}}^{T_{\mathrm{p,max}}} r(T_{\mathrm{p}},t|z,\boldsymbol{\theta})n(z,t)\,\mathrm{d}zF_{\boldsymbol{\theta}}(\mathrm{d}\boldsymbol{\theta},t) \\
&\quad = q_{\mathrm{p}}(t)n_{\mathrm{in}}(T_{\mathrm{p}},t)-q_{\mathrm{p}}(t)n(T_{\mathrm{p}},t)
\end{aligned} \tag{4}
$$

where it was assumed that the feed and withdrawal rates of particles do not depend on the particle population itself and have no random components.

Since the population density function of the wall is, in principle, the density function of a degenerate distribution thus the population balance equation for that, i.e. the counterpart of Eq. (1) for the "second population" could be given only in weak formulation. Therefore, the population balance equation for the wall is written as

$$\left\langle \varphi, \frac{\partial n_{\rm w}(T,t)}{\partial t} \right\rangle = -\left\langle \varphi, \frac{\partial}{\partial T}(G_T^{\rm wg} n_{\rm w}(T,t)) \right\rangle - \left\langle \varphi, \frac{\partial}{\partial T}(G_T^{\rm wl} n_{\rm w}(T,t)) \right\rangle$$
$$- \left\langle \varphi, \int_{\Omega_{\rm wp}} \int_{T_{\rm p,min}}^{T_{\rm p,max}} \int_{T_{\rm w,min}}^{T_{\rm w,max}} S_{\rm wp}(T_{\rm w}|z) b_{\rm wp}(T_{\rm w}, y|z, \omega_{\rm wp}) \times n_{\rm w}(T,t) n(z,t)\, {\rm d}z\, {\rm d}y F_{\omega_{\rm wp}}({\rm d}\omega_{\rm wp}) \right\rangle$$
$$+ \left\langle \varphi, \int_{\Omega_{\rm wp}} \int_{T_{\rm p,min}}^{T_{\rm p,max}} \int_{T_{\rm w,min}}^{T_{\rm w,max}} S_{\rm wp}(y|z) b_{\rm wp}(y, T|z, \omega_{\rm wp}) \times n_{\rm w}(y,t) n(z,t)\, {\rm d}y\, {\rm d}z F_{\omega_{\rm wp}}({\rm d}\omega_{\rm wp}) \right\rangle \quad (5)$$

where φ is some smooth function of variable T with a compact support, and $\langle .,. \rangle$ denotes the scalar product in the appropriate function space. $G_T^{\rm wg}$ and $G_T^{\rm wl}$ are continuous rates of change of the wall temperature due to gas–wall and wall–liquid environment heat transfers, respectively, while the third and fourth terms on the right hand side of Eq. (5) describe the variation of the wall temperature induced by collisional heat transfer between the wall and particles.

In order to close these model equations the constitutive expressions for the activity functions $S_{\rm pp}$, $S_{\rm pw}$ and $S_{\rm wp}$, as well as for the conversion density functions $b_{\rm pp}$, $b_{\rm pw}$ and $b_{\rm wp}$ have to be determined.

3. Constitutive expressions

The activity functions $S_{\rm pp}$, $S_{\rm pw}$ and $S_{\rm wp}$ which characterise the intensities of particle–particle and particle–wall interactions are, in principle, products of the collision frequencies $S_{\rm pp}^{\rm col}(T|T'), S_{\rm pw}^{\rm col}(T|T')$ and $S_{\rm wp}^{\rm col}(T|T')$, and heat exchange terms $S_{\rm pp}^{\rm ex}(T|T'), S_{\rm pw}^{\rm ex}(T|T')$ and $S_{\rm wp}^{\rm ex}(T|T')$. Here, the heat exchange terms express the ratios of collisions of two bodies in which the collision event is associated with equalization event of temperatures. In other words, the heat exchange terms characterise the efficiency of collisions with respect to heat transfer between the colliding bodies. Since heat transfer deciding at this level on homogenisation of temperature is a spontaneous process, i.e. it occurs in each collision to some extent, thus the heat exchange terms equal to unity identically: $S_{\rm pp}^{\rm ex}(T|T') = S_{\rm pw}^{\rm ex}(T|T') = S_{\rm wp}^{\rm ex}(T|T') \equiv 1$. As a consequence, $S_{\rm pp}(T|T') = S_{\rm pp}^{\rm col}(T|T')$ and $S_{\rm pw}(T|T') = S_{\rm wp}(T|T') = S_{\rm pw}^{\rm col}(T|T')$. Note that the collision frequency may depend on the temperature indirectly through the temperature dependence of the density and viscosity of the gas phase.

In order to develop the conversion density functions $b_{\rm pp}$, $b_{\rm pw}$ and $b_{\rm wp}$ we consider an encounter of two solid bodies of mass m_j and m_k, temperatures T_j and T_k, and heat capacities c_j and c_k. If these bodies collide at moment of time $t = 0$ and remain in contact for some time θ then some heat exchange occurs between them as it shown in Fig. 3. Assuming that this heat transfer can be described by the heat transfer coefficient h then the equations describing the variation of temperatures of bodies are:

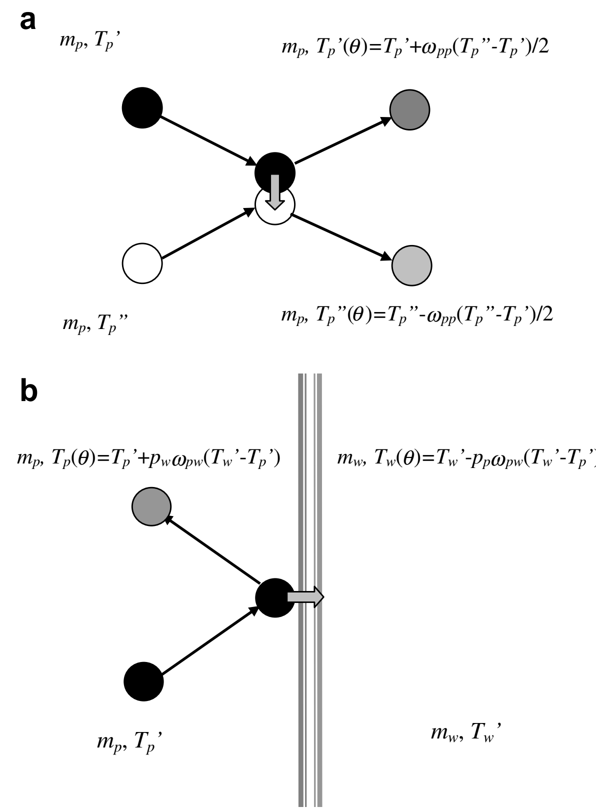

Fig. 3. Illustrations for collisional heat transfers (a) between two particles, and (b) between a particle and the wall.

$$m_j c_j \frac{{\rm d}T_j(t)}{{\rm d}t} = ha(T_k(t) - T_j(t)) \quad (6)$$

$$m_k c_k \frac{{\rm d}T_k(t)}{{\rm d}t} = -ha(T_k(t) - T_j(t)) \quad (7)$$

subject to the initial conditions

$$T_j(0) = T_{j0}, \quad T_k(0) = T_{k0} \quad (8)$$

The solutions of the first order differential equations (6) and (7) at time θ become

$$T_j(\theta) = T_{j0} + \frac{m_k c_k}{m_j c_j + m_k c_k}(T_{k0} - T_{j0}) \times \left\{1 - \exp\left[-ha\theta\left(\frac{1}{m_j c_j} + \frac{1}{m_k c_k}\right)\right]\right\} = T_{j0} + p_j \omega (T_{k0} - T_{j0}) \quad (9)$$

$$T_k(\theta) = T_{k0} - \frac{m_j c_j}{m_j c_j + m_k c_k}(T_{k0} - T_{j0}) \times \left\{1 - \exp\left[-ha\theta\left(\frac{1}{m_j c_j} + \frac{1}{m_k c_k}\right)\right]\right\} = T_{k0} - p_k \omega (T_{k0} - T_{j0}) \quad (10)$$

where

$$\omega := 1 - \exp\left[-ha\theta\left(\frac{m_j c_j + m_k c_k}{m_j c_j m_k c_k}\right)\right],$$

$$p_j = \frac{m_k c_k}{m_j c_j + m_k c_k} \quad \text{and} \quad p_k = \frac{m_j c_j}{m_j c_j + m_k c_k}.$$

In Eqs. (9) and (10), parameters h, a and θ are, in principle, random quantities since the quality and area of contact, as well as the contact time in such collisions may depend on a number of random conditions. Indeed, this transfer process is a combination of conduction through the contact point and through the gas lens around the contact point, which depend on the shapes and velocities of the colliding bodies. As a consequence parameter $\omega \in [0,1]$, characterising the efficiency of heat exchange between the colliding bodies is a random function of the parameters h, a and θ, and its distribution is entirely determined by their distribution functions. The changes of temperatures of the bodies induced by the collisions are given by Eqs. (9) and (10), respectively.

Let us now assume that the two bodies suffering collisions are two particles with equal masses and heat capacities. Then, $m_j c_j = m_k c_k = m_\mathrm{p} c_\mathrm{p}$ and $p_j = p_k = \frac{1}{2}$. Introducing the notation $T_{j0} = T'_\mathrm{p}$, $T_{k0} = T''_\mathrm{p}$ we can write

$$\omega := \omega_\mathrm{pp} = 1 - \exp\left[\frac{-2h_\mathrm{pp}a_\mathrm{pp}\theta_\mathrm{pp}}{m_\mathrm{p}C_\mathrm{p}}\right] \quad \text{and}$$

$$T_\mathrm{p}(\theta) = T'_\mathrm{p} + (T''_\mathrm{p} - T'_\mathrm{p}) \cdot \frac{\omega_\mathrm{pp}}{2} \tag{11}$$

from which

$$\frac{2\left(T_\mathrm{p} - T'_\mathrm{p}\right)}{\omega_\mathrm{pp}} + T'_\mathrm{p} = T''_\mathrm{p}. \tag{12}$$

Interpretation of Eq. (12) is that in heat transfer process characterised with parameter ω_pp a particle with temperature T'_p has to collide with particle of temperature T''_p to achieve final temperature T_p. Taking now into consideration the definitions of conversion functions, the conversion distribution function of particle–particle heat transfer takes the form

$$B_\mathrm{pp}(T'_\mathrm{p}, T_\mathrm{p}|T''_\mathrm{p}, \omega_\mathrm{pp}) = \mathbf{1}_{T_\mathrm{p}}\left[\left(\frac{2\left(T_\mathrm{p} - T'_\mathrm{p}\right)}{\omega_\mathrm{pp}} + T'_\mathrm{p}\right) - T''_\mathrm{p}\right] \tag{13}$$

so that the corresponding density function is

$$b_\mathrm{pp}(T'_\mathrm{p}, T_\mathrm{p}|T''_\mathrm{p}, \omega_\mathrm{pp}) = \delta_{T_\mathrm{p}}\left[\left(\frac{2\left(T_\mathrm{p} - T'_\mathrm{p}\right)}{\omega_\mathrm{pp}} + T'_\mathrm{p}\right) - T''_\mathrm{p}\right]\frac{2}{\omega_\mathrm{pp}}. \tag{14}$$

When a particle and the wall are two colliding bodies, as it shown in Fig. 3b, then denoting $m_j c_j = m_\mathrm{p} c_\mathrm{p}$, $m_k c_k = m_\mathrm{w} c_\mathrm{w}$, $p_j = p_\mathrm{p} = \frac{m_\mathrm{w}c_\mathrm{w}}{m_\mathrm{p}c_\mathrm{p}+m_\mathrm{w}c_\mathrm{w}}$, $p_k = p_\mathrm{w} = \frac{m_\mathrm{p}c_\mathrm{p}}{m_\mathrm{p}c_\mathrm{p}+m_\mathrm{w}c_\mathrm{w}}$, $T_{j0} = T'_\mathrm{p}$ and $T_{k0} = T'_\mathrm{w}$ we can write

$$\omega := \omega_\mathrm{pw} = \omega_\mathrm{wp} = 1 - \exp\left[\frac{-h_\mathrm{pw}a_\mathrm{pw}\theta_\mathrm{pw}\left(m_\mathrm{p}c_\mathrm{p} + m_\mathrm{w}c_\mathrm{w}\right)}{m_\mathrm{p}c_\mathrm{p}m_\mathrm{w}c_\mathrm{w}}\right]. \tag{15}$$

Expression (10) is written as

$$T_\mathrm{p}(\theta) = p_\mathrm{w}\omega_\mathrm{pw}(T'_\mathrm{w} - T'_\mathrm{p}) + T'_\mathrm{p} \tag{16}$$

from which

$$\frac{T_\mathrm{p} - T'_\mathrm{p}}{p_\mathrm{w}\omega_\mathrm{pw}} + T'_\mathrm{p} = T'_\mathrm{w}. \tag{17}$$

Eq. (17) expresses the fact that in heat transfer process between a particle and the wall, characterised with parameter ω_pw, the temperature T'_p of the particle becomes T_p if the temperature of the wall was T'_w. As a consequence, the conversion distribution function of the particle–wall heat transfer for particles takes the form

$$B_\mathrm{pw}(T'_\mathrm{p}, T_\mathrm{p}|T'_\mathrm{w}, \omega_\mathrm{pw}) = \mathbf{1}_{T_\mathrm{p}}\left[\left(\frac{T_\mathrm{p} - T'_\mathrm{p}}{p_\mathrm{w}\omega_\mathrm{pw}} + T'_\mathrm{p}\right) - T'_\mathrm{w}\right] \tag{18}$$

thus the density function becomes

$$b_\mathrm{pw}(T'_\mathrm{p}, T_\mathrm{p}|T''_\mathrm{w}, \omega_\mathrm{pw}) = \delta_{T_\mathrm{p}}\left[\left(\frac{T_\mathrm{p} - T'_\mathrm{p}}{p_\mathrm{w}\omega_\mathrm{pw}} + T'_\mathrm{p}\right) - T'_\mathrm{w}\right]\frac{1}{p_\mathrm{w}\omega_\mathrm{pw}}. \tag{19}$$

Finally, in the particle–wall collisional heat transfer we consider the process from the side of the wall. Now expression (10) is rewritten as

$$\frac{T_\mathrm{w} - T'_\mathrm{w}}{p_\mathrm{p}\omega_\mathrm{pw}} + T'_\mathrm{w} = T'_\mathrm{p}. \tag{20}$$

based on which, since the change of the wall temperature is related to $T_\mathrm{w}(t)$ which is fixed at the moment t the conversion distribution function becomes

$$B_\mathrm{wp}(T'_\mathrm{w}, T_\mathrm{w}|T'_\mathrm{p}, \omega_\mathrm{wp}) = \mathbf{1}_{T_\mathrm{w}}\left[\left(\frac{T_\mathrm{w} - T'_\mathrm{w}}{p_\mathrm{p}\omega_\mathrm{wp}} + T'_\mathrm{w}\right) - T'_\mathrm{p}\right] \tag{21}$$

while the conversion density function

$$b_\mathrm{wp}(T'_\mathrm{w}, T_\mathrm{w}|T'_\mathrm{p}, \omega_\mathrm{wp}) = \delta_{T_\mathrm{w}}\left[\left(\frac{T_\mathrm{w} - T'_\mathrm{w}}{p_\mathrm{p}\omega_\mathrm{wp}} + T'_\mathrm{w}\right) - T'_\mathrm{p}\right]\frac{1}{p_\mathrm{p}\omega_\mathrm{wp}}. \tag{22}$$

At this moment all constitutive expressions of Eqs. (1) and (5) have been derived and the heat balance model of the process, applying the population balance equations (1) and (5) can be determined.

4. Population balance model

Let us assume that the collision frequencies, depending on the hydrodynamic and load conditions, are constant. Then, substituting the conversion density functions (14) and (19) into Eq. (1), taking into account relations (3) and (4) and the properties of Dirac-delta function we obtain

$$\frac{\partial n(T_p,t)}{\partial t} = -\frac{\partial}{\partial T_p}[K_{pg}(T_g(t)-T_p)n(T_p,t)] + \frac{q_p}{V}(n_{in}(T_p,t) - n(T_p,t)) - (S_{pp}+S_{pw})n(T_p,t) + \int_{\Omega_{pp}} \frac{2S_{pp}}{\omega_{pp}} \frac{1}{N(t)} \int_{T_{p,min}}^{T_{p,max}} \int_{T_{p,min}}^{T_{p,max}} \delta\left[\left(\frac{2(T_p-y)}{\omega_{pp}}+y\right)-z\right] \times n(y,t)n(z,t)\,dy\,dzF_{\omega_{pp}}(d\omega_{pp}) + \int_{\Omega_{pw}} \frac{S_{pw}}{p_w\omega_{pw}} \int_{T_{w,min}}^{T_{w,max}} \int_{T_{p,min}}^{T_{p,max}} \delta\left[\left(\frac{T_p-y}{p_w\omega_{pw}}+y\right)-z\right] \times n(y,t)\,dy\,n_w(z,t)\,dzF_{\omega_{pw}}(d\omega_{pw}) \tag{23}$$

The heat balance equation for the wall is derived from Eq. (5) where the power functions T^k, $k=0,1,2,\ldots$ can be selected as test functions φ in the compact interval $[T_{w,min}, T_{w,max}]$ leading to the moments of the Dirac-delta function representing the "population density function" of the wall:

$$\langle T^k, \delta[T-T_w(t)]\rangle = \int_{T_{w,min}}^{T_{w,max}} T^k\delta[T-T_w(t)]\,dT, \quad k=0,1,2,\ldots \tag{24}$$

from which the first order moment provides the wall temperature T_w.

The first term on the right hand side of Eq. (5), describing the continuous gas–wall heat transfer with linear force becomes

$$\left\langle T, \frac{\partial}{\partial T}(G_T^{wg}(T)\delta[T-T_w(t)])\right\rangle = \int_{T_{w,min}}^{T_{w,max}} T\frac{\partial}{\partial T}(G_T^{wg}(T)\delta[T-T_w(t)])\,dT = TG_T^{wg}(T)\delta[T-T_w(t)]\Big|_{T_{w,min}}^{T_{w,max}} - \int_{T_{w,min}}^{T_{w,max}} G_T^{wg}(T)\delta[T-T_w(t)]\,dT = -G_T^{wg}[T_w(t)] \tag{25}$$

that generates in the interval of time $(t, t+dt)$

$$dQ_{wg} = h_{wg}a_{wg}(T_g(t)-T_w(t))\,dt \tag{26}$$

change in the heat absorbed by the wall. The effect of the wall–environment heat transfer can be formulated similarly what provides the expression

$$dQ_{wl} = -h_{wl}a_{wl}(T_w(t)-T_l(t))\,dt \tag{27}$$

for that case.

As regards the effects of the particle–wall heat transfer, particle–wall collisions induce small jump-like changes in the wall temperature the results of which for the whole population are expressed by the mean temperature of the wall as

$$-\left\langle T, \int_{\Omega_{wp}} \int_{T_{p,min}}^{T_{p,max}} \int_{T_{w,min}}^{T_{w,max}} S_{wp}(T_w|z)b_{wp}(T_w,y|z,\omega_{wp}) \times n(z,t)\,dz\,n_w(T,t)\,dyF_{\omega_{wp}}(d\omega_{wp})\right\rangle + \left\langle T, \int_{\Omega_{wp}} \int_{T_{p,min}}^{T_{p,max}} \int_{T_{w,min}}^{T_{w,max}} S_{wp}(y|z)b_{wp}(y,T|z,\omega_{wp}) \times n(z,t)\,dz\,n_w(y,t)\,dyF_{\omega_{wp}}(d\omega_{wp})\right\rangle \tag{28}$$

Substituting expression (22) for b_{wp} into Eq. (28) and rearranging we obtain

$$-\left\langle T, \int_{\Omega_{wp}} S_{wp} \int_{T_{p,min}}^{T_{p,max}} \int_{T_{w,min}}^{T_{w,max}} \delta\left[\left(\frac{y-T_w}{p_p\omega_{wp}}+T_w\right)-z\right] \times \frac{1}{p_p\omega_{wp}} n(z,t)\,dzn_w(T,t)\,dyF_{\omega_{wp}}(d\omega_{wp})\right\rangle + \left\langle T, \int_{\Omega_{wp}} S_{wp} \int_{T_{p,min}}^{T_{p,max}} \int_{T_{w,min}}^{T_{w,max}} \delta\left[\left(\frac{T-y}{p_p\omega_{wp}}+y\right)-z\right] \times \frac{1}{p_p\omega_{wp}} n(z,t)\,dz\,n_w(y,t)\,dyF_{\omega_{wp}}(d\omega_{wp})\right\rangle = \int_{\Omega_{wp}} S_{wp}p_p\omega_{wp} \int_{T_{p,min}}^{T_{p,max}} (T_p - T_w(t))n(T_p,t)\,dT_pF_{\omega_{wp}}(d\omega_{wp}) = -S_{wp}p_p m_{1,\omega_{wp}}(T_w(t)M_0(t) - M_1(t)) \tag{29}$$

From the other side, collision of a particle of temperature T_p with the wall of temperature T_w induces change of value $m_w c_w p_p \omega_{pw}(T_p - T_w(t))$ in the heat of the wall so that the total amount of heat exchanged between the wall and particles of a unit volume of suspension is expressed as

$$dQ_{wp} = m_w c_w S_{wp} p_p \omega_{wp}(T_p - T_w(t))n(T_p,t)\,dT_p\,dt. \tag{30}$$

As a consequence, the heat balance equation for the wall takes the form

$$m_w c_w \frac{dT_w(t)}{dt} = h_{wg}a_{wg}V\varepsilon(T_g(t)-T_w(t)) - h_{wl}a_{wl}V_l(T_w(t)-T_l(t)) - VS_{wp}m_w c_w \int_{\Omega_{pw}} \int_{T_{p,min}}^{T_{p,max}} p_p\omega_{wp}(T_p-T_w(t))n(T_p,t)\,dT_pF_{\omega_{wp}}(d\omega_{wp}) \tag{31}$$

where the first and second terms on the right hand side describe the total heat fluxes between the wall and the gas and liquid, respectively, while the last term represents the total heat flux between the entire population of particles and the wall.

The heat flux between the gas and particles taken from the temperature interval $(T_p, T_p + dT_p)$ in a unit volume of suspension at time t is expressed as

$$h_{pg}a_{pg}(T_g(t)-T_p)n(T_p,t)\,dT_p \tag{32}$$

where $h_{pg}a_{pg}(T_g(t) - T_p)$ denotes the heat flux between a single particle and the gas. Therefore, the total heat transfer between the gas and the entire particle population immersed in gas is given as

$$Vh_{pg}a_{pg}\int_{T_{p,\min}}^{T_{p,\max}}(T_g(t) - T_p(t))n(T_p,t)\,dT_p. \tag{33}$$

so that the heat balance equation for the gas phase takes the form

$$\begin{aligned} V\rho_g c_g \varepsilon \frac{dT_g(t)}{dt} &= q_g\rho_g c_g(T_{g,in}(t) - T_g(t)) - h_{wg}a_{wg}V\varepsilon(T_g(t) - T_w(t)) \\ &\quad - Vh_{pg}a_{pg}\int_{T_{p,\min}}^{T_{p,\max}}(T_g(t) - T_p)n(T_p,t)\,dT_p \end{aligned} \tag{34}$$

where the first term on the right hand side describes the input–output process, the second and third terms, representing, respectively, the gas–wall and gas–particle population heat transfer fluxes are of the forms given by Eqs. (26) and (33).

Finally, based on similar considerations as Eq. (34), the heat balance equation for the cooling or heating medium playing the role of the environment of the system takes the form

$$V_1\rho_1 c_1\frac{dT_1(t)}{dt} = q_1\rho_1 c_1(T_{l,in}(t) - T_1(t)) - h_{wl}a_{wl}V_1(T_1(t) - T_w(t)). \tag{35}$$

The set of Eqs. (23), (31), (34) and (35) subject to the boundary conditions

$$(G_T^{pg}n(T_p,t))|_{T_{p,\min+}} = 0 \quad \text{and} \quad (G_T^{pg}n(T_p,t))|_{T_{p,\max-}} = 0 \tag{36}$$

and the initial conditions

$$n(T_p,0) = n_0(T_p), \quad T_w(0) = T_{w0}, \quad T_g(0) = T_{g0}, \quad T_1(0) = T_{10} \tag{37}$$

provides the population balance model of heat transfer processes of the system. In order to investigate the properties of the model by means of simulation next the moment equation model will be derived for the moments of temperature of the particle population.

5. Moment equation model

Introducing the moments of the temperature of particle population, expressed as

$$M_k(t) = \int_{T_{p,\min}}^{T_{p,\max}} T_p^k n(T_p,t)\,dT_p, \quad k = 0,1,2,\ldots \tag{38}$$

we can derive an infinite set of the moment equations of the system. Indeed, multiplying both sides of Eq. (23) by T_p^k, $k = 0,1,2\ldots$ and integrating over the interval $[T_{p,\min}, T_{p,\max}]$ after some suitable transformations we get the following system of ordinary differential equations:

$$\begin{aligned} \frac{dM_k(t)}{dt} &= \frac{q_p}{V}(M_{k,in}(t) - M_k(t)) + kK_{pg}(M_{k-1}(t)T_g(t) - M_k(t)) \\ &\quad + \frac{S_{pp}}{M_0(t)}\sum_{j=0}^{k} b_{j,k}^{pp}M_j(t)M_{k-j}(t) + S_{pw}\sum_{j=0}^{k} b_{j,k}^{pw}M_j(t)T_w^{k-j}(t), \\ &\quad k = 0,1,2,\ldots \end{aligned} \tag{39}$$

subject to the initial conditions

$$M_k(0) = M_{k,0}, \quad k = 0,1,2,\ldots \tag{40}$$

where

$$b_{j,k}^{pp} = \int_0^1 \binom{k}{j}\left(\frac{\omega_{pp}}{2}\right)^j\left(1 - \frac{\omega_{pp}}{2}\right)^{k-j}F_{\omega_{pp}}(d\omega_{pp}), \quad k = 0,1,2,\ldots, j = 1,2,\ldots k \tag{41}$$

$$b_{j,k}^{pw} = \int_0^1 \binom{k}{j}(1 - p_w\omega_{pw})^j(p_w\omega_{pw})^{k-j}F_{\omega_{pw}}(d\omega_{pw}), \quad k = 0,1,2,\ldots, j = 1,2,\ldots k \tag{42}$$

As a consequence, the equations of the moment equation model for the wall, gas and the environment are written as:

$$\frac{dT_g(t)}{dt} = \frac{q_g}{V\varepsilon}(T_{g,in}(t) - T_g(t)) - \frac{h_{wg}a_{wg}}{\rho_g c_g}(T_g(t) - T_w(t)) - \frac{h_{pg}a_{pg}}{\rho_g c_g\varepsilon}(M_0(t)T_g(t) - M_1(t)) \tag{43}$$

$$\frac{dT_w(t)}{dt} = \frac{h_{wg}a_{wg}V\varepsilon}{m_w c_w}(T_f(t) - T_w(t)) - \frac{h_{wl}a_{wl}V_1}{m_w c_w}(T_w(t) - T_1(t)) - VS_{wp}p_p m_{1,\omega_{wp}}(M_1(t) - M_0(t)T_w(t)) \tag{44}$$

$$\frac{dT_1(t)}{dt} = \frac{q_1}{V_1}(T_{l,in}(t) - T_1(t)) - \frac{h_{wl}a_{wl}}{\rho_1 c_1}(T_1(t) - T_w(t)). \tag{45}$$

The set of moment equations (39) form an infinite hierarchy, but, due to the linear nature of the rate of changes of the particle temperature, this set can be closed at any order so that the moment equation model consisting of Eqs. (39), (43), (44) and (45) is, in principle, closed. However, for computing the heat balance Eqs. (43)–(45) we need only the zero and first order moments while the second and higher order moments can be used to characterise the temperature distribution of particles. Here, the set of recursive differential equation (39) is closed at the second order moment, deriving in this way a second order moment equation model for analysing the total heat balance of gas–solid system and the variance of the temperature of particle population:

$$\frac{\mathrm{d}M_0(t)}{\mathrm{d}t} = \frac{q_\mathrm{p}}{V}(M_{0,\mathrm{in}}(t) - M_0(t)) \tag{46}$$

$$\frac{\mathrm{d}M_1(t)}{\mathrm{d}t} = \frac{q_\mathrm{p}}{V}(M_{1,\mathrm{in}}(t) - M_1(t)) + K_{\mathrm{pg}}(M_0(t)T_\mathrm{g}(t) - M_1(t)) + S_{\mathrm{pw}}p_\mathrm{w}m_{1,\omega_{\mathrm{pw}}}(M_1(t) - T_\mathrm{w}(t)M_0(t)) \tag{47}$$

$$\frac{\mathrm{d}M_2(t)}{\mathrm{d}t} = \frac{q_\mathrm{p}}{V}(M_{2,\mathrm{in}}(t) - M_2(t)) + 2K_{\mathrm{pg}}(M_1(t)T_\mathrm{g}(t) - M_2(t)) + S_{\mathrm{pp}}\kappa_{\mathrm{pp}}\left(\frac{M_1^2(t)}{M_0(t)} - M_2(t)\right) + 2S_{\mathrm{pw}}p_\mathrm{w}m_{1,\omega_{\mathrm{pw}}}(T_\mathrm{w}(t)M_1(t) - M_2(t)) + S_{\mathrm{pw}}p_\mathrm{w}^2 m_{2,\omega_{\mathrm{pw}}}(M_2(t) - 2T_\mathrm{w}(t)M_1(t) + T_\mathrm{w}^2(t)M_0(t)) \tag{48}$$

where the coefficients of terms representing the collisional particle–particle and particle–wall heat transfers are expressed by means of expectations and variances of random parameters ω_{pp} and ω_{pw}. In Eq. (48), we have

$$\kappa_{\mathrm{pp}} = m_{1,\omega_{\mathrm{pp}}}\left(1 - \frac{m_{1,\omega_{\mathrm{pp}}}}{2}\right) - \frac{\sigma^2_{\omega_{\mathrm{pp}}}}{2}. \tag{49}$$

In assessing the simulation results, often the normalised moments are used which can be computed from moments (39) as

$$m_k(t) = \frac{M_k(t)}{M_0(t)}, \quad k = 0, 1, 2 \ldots \tag{50}$$

Here, the first order moment $m_1(t)$ provides the mean temperature of the particle population. Besides, knowing the first three leading moments the variance of the temperature of particle population, characterising the temperature distribution of particles and expressed as

$$\sigma^2(t) = \frac{M_2(t)}{M_0(t)} - \left(\frac{M_1(t)}{M_0(t)}\right)^2 = m_2(t) - m_1^2(t) \tag{51}$$

will be used.

6. Simulation results and discussion

The frequencies of particle–particle and particle–wall collisions depend on the void fraction of the bed, the particle size and the velocity of particles. Under steady hydrodynamic conditions the particle velocities depend to some extent on the temperature through the temperature dependence of the density and viscosity of the carrier medium but this effect under given operational conditions is considered to be negligible. From the other side, the velocity of particles is a fluctuating quantity hence the frequencies of interparticle and particle–wall collisions are characterised by probability distributions either according to the kinetic theory [20,24] or to experimentally derived distributions [21–23]. Taking into account this influence by randomization of the integral terms in Eq. (1) gives again constant frequencies under given hydrodynamic conditions since these quantities are not correlated with the remaining variables in the integrals.

In numerical experiments, the hydrodynamic properties of the fluidized bed were computed using correlations given by Eqs. (T1) and (T2), listed in Table 1, while the gas–wall, wall–liquid and gas–particle heat transfer coefficients, all based on physical properties of materials and the void fraction of the bed were computed using Eqs. (T3)–(T5), also listed in Table 1.

The values of process parameters were taken constant using their basic values shown in Tables 2 and 3 except the parameter the effects of which on the heat transfer processes were actually examined.

Table 2
Basic values of physical and thermal parameter used in numerical experiments

	Parameter	Basic value
Solid particle: *alumina*	Diameter, d_p	1.8×10^{-3} m
	Density, ρ_p	1040 kg m^{-3}
	Specific heat, c_p	944 J kg^{-1} K^{-1}
	Thermal conductivity, k_p	36 W m^{-1} K^{-1}
Gas: *air*	Density, ρ_g	0.946 kg m^{-3}
	Specific heat, c_g	1010 J kg^{-1} K^{-1}
	Viscosity, μ_g	2.17×10^{-5} Pa s
	Thermal conductivity, k_g	2.39×10^{-2} W m^{-1} K^{-1}
Wall: *stainless steel*	Mass, m_w	145 kg
	Specific heat, c_w	465 J kg^{-1} K^{-1}
	Thermal conductivity, k_w	50.2 W m^{-1} K^{-1}
Wall: *glass*	Mass, m_w	47 kg
	Specific heat, c_w	503 J kg^{-1} K^{-1}
	Thermal conductivity, k_w	0.8 W m^{-1} K^{-1}
Cooling medium: *water*	Density, ρ_l	998 kg m^{-3}
	Specific heat, c_l	4182 J kg^{-1} K^{-1}
	Thermal conductivity, k_l	0.606 W m^{-1} K^{-1}
	Viscosity, μ_l	1.0×10^{-3} Pa s

Table 1
Correlations for hydrodynamic and heat transfer parameters used in numerical experiments

Correlation	Source	Equation
$Re_{mf} = (33.7^2 + 0.0408Ar)^{1/2} - 33.7$	Wen and Yu [25]	(T1)
$\frac{1}{Re_t} = \frac{21.35}{\log\left(\frac{\varepsilon}{0.065}\right)}\frac{1}{Ar} + \sqrt{\frac{2.78-2.556\varepsilon}{Ar}}$	Gumz and Frössling In [26]	(T2)
$Nu_{\mathrm{gw}} = 0.0175Ar^{0.46}Pr_\mathrm{g}^{0.33}$	Baskakov and Suprun [27]	(T3)
$Nu_{\mathrm{lw}} = 0.023Re_{lw}^{0.8}Pr_\mathrm{l}^{0.3}$	Dittus–Boelter Correlation	(T4)
$Nu_\mathrm{p} = 0.054\left(\frac{Re_\mathrm{p}}{\varepsilon}\right)^{1.28}$	Richardson and Ayers [28]	(T5)

Table 3
Basic values of operating parameters used in numerical experiments

	Parameter	Basic value
Fluidized bed	Diameter, D	0.65 m
	Height, H	0.9 m
	Particle volumetric flow rate, q_p	$1.0 \times 10^{-3}\ \mathrm{m}^3\ \mathrm{s}^{-1}$
	Gas volumetric flow rate, q_g	$1.2 \times 10^{-1}\ \mathrm{m}^3\ \mathrm{s}^{-1}$
Gas–solid suspension	Void fraction, ε	0.6
Cooling jacket	Diameter, D_l	0.75 m
	Water volumetric flow rate, q_l	$1.0 \times 10^{-3}\ \mathrm{m}^3\ \mathrm{s}^{-1}$

Since the support of random parameters ω_{pp} and ω_{pw} is the compact interval $[0,1]$ these parameters were characterised by the beta distribution

$$f_{\omega_\iota}(\omega) = \begin{cases} \frac{1}{\beta(p,q)}\omega_\iota^{p-1}(1-\omega_\iota)^{q-1}, \\ \quad \text{if } 0 < \omega_\iota < 1, \\ 0, \quad \text{if } 0 \leqslant \omega_\iota \text{ and if } \omega_\iota \geqslant 1 \end{cases} \qquad \iota = \mathrm{pp}, \mathrm{pw} \tag{52}$$

including also the limiting degenerate distributions formed by Dirac-delta density functions.

The input was generated as a step function of particles of number $\phi M_{0,\mathrm{in}}$ and $(1-\phi)M_{0,\mathrm{in}}$, $0 \leqslant \phi \leqslant 1$, having two different temperatures $T_{\mathrm{p,in}}^{(1)}$ and $T_{\mathrm{p,in}}^{(2)}$, respectively, which were totally segregated from each other as it is illustrated in Fig. 4a. Such temperature distribution is described by the population distribution function

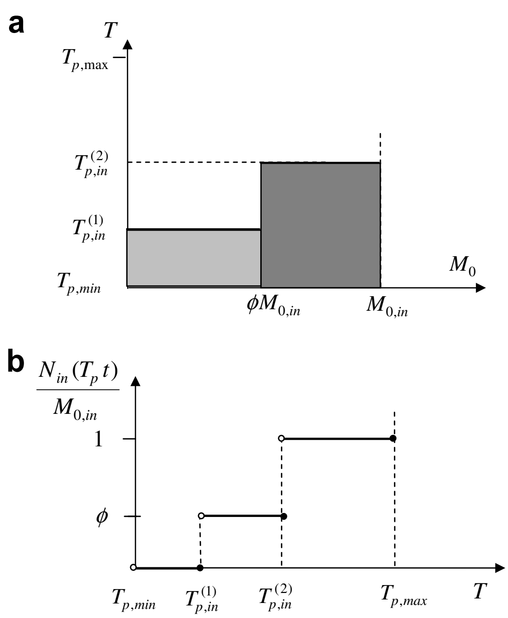

Fig. 4. (a) The input population of particles of two different temperatures mixed in ratio ϕ, and (b) the corresponding population distribution function of temperature.

$$N_{\mathrm{in}}(T_{\mathrm{p}}, t) = \phi M_{0,\mathrm{in}}\mathbf{1}(T_{\mathrm{p}} - T_{\mathrm{p,in}}^{(1)}) + (1-\phi)M_{0,\mathrm{in}}\mathbf{1}(T_{\mathrm{p}} - T_{\mathrm{p,in}}^{(2)}), \quad 0 \leqslant \phi \leqslant 1 \tag{53}$$

shown in Fig. 4b from which the input population density function has the form

$$n_{\mathrm{in}}(T_{\mathrm{p}}, t) = \phi M_{0,\mathrm{in}}\delta(T_{\mathrm{p}} - T_{\mathrm{p,in}}^{(1)}) + (1-\phi)M_{0,\mathrm{in}}\delta(T_{\mathrm{p}} - T_{\mathrm{p,in}}^{(2)}), \quad 0 \leqslant \phi \leqslant 1. \tag{54}$$

As a consequence, the mean value and variance of the temperature of input particle population are given as

$$m_{1,\mathrm{in}} = \phi T_{\mathrm{p,in}}^{(1)} + (1-\phi)T_{\mathrm{p,in}}^{(2)} \quad \text{and}$$
$$\sigma_{\mathrm{in}}^2 = m_2 - m_1^2 = \phi(1-\phi)(T_{\mathrm{p,in}}^{(1)} - T_{\mathrm{p,in}}^{(2)})^2. \tag{55}$$

The orders of magnitudes of the frequencies of particle–particle and particle–wall collisions, given as $S_{\mathrm{pp}} = \boldsymbol{O}(10) \div \boldsymbol{O}(100)$ and $S_{\mathrm{pw}} = \boldsymbol{O}(1)$ respectively, were chosen according to the experimental data reported by Sommerfeld [20,21] and Hamidipouret al. [22,23].

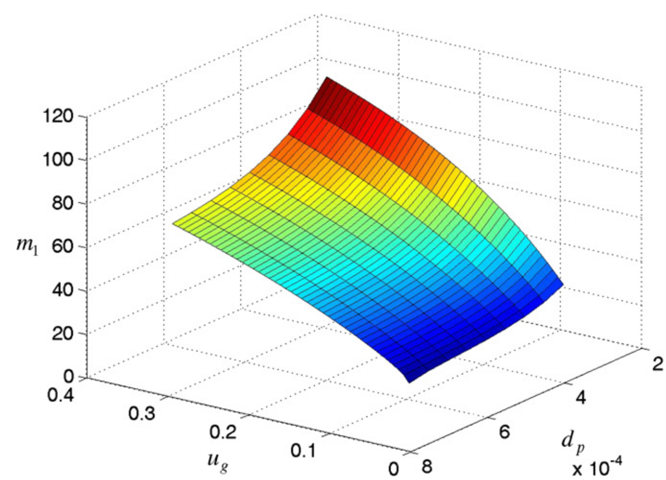

Fig. 5. The mean temperature of particle population as a function of the gas velocity and particle diameter.

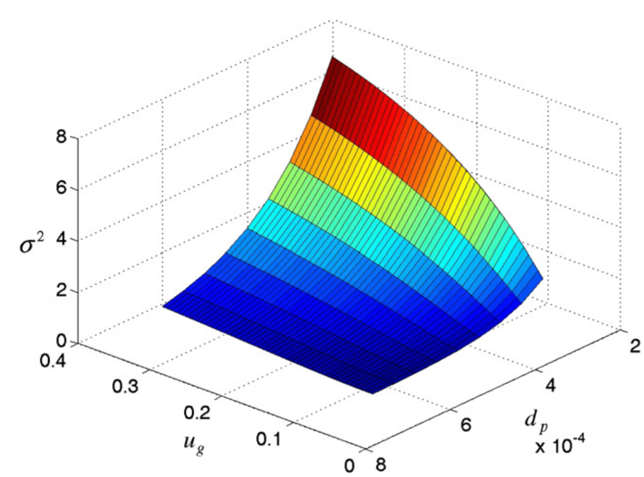

Fig. 6. The variance of temperature of the particle population as a function of the gas velocity and particle diameter.

Numerical experimentation was carried out in MATLAB environment by developing computer programs for solving the set of ordinary differential equations (43)–(45), (45)–(48) using the ODE solver ode15s of MATLAB.

The mean temperature of particles as a function of the gas velocity and particle diameter is shown in Fig. 5, while the dependence of the variance of temperature of particles, obtained under the same operational conditions, and, in essence, characterising the temperature inhomogeneities of the particle population is seen in Fig. 6.

With increasing gas temperature the mean temperature of particles is increased but, simultaneously, the variance of temperature of the particle population. i.e. the temperature inhomogeneities of particles become also increased. This unfavourable effect of increased variance is reduced by the collisional particle–particle and particle–wall heat

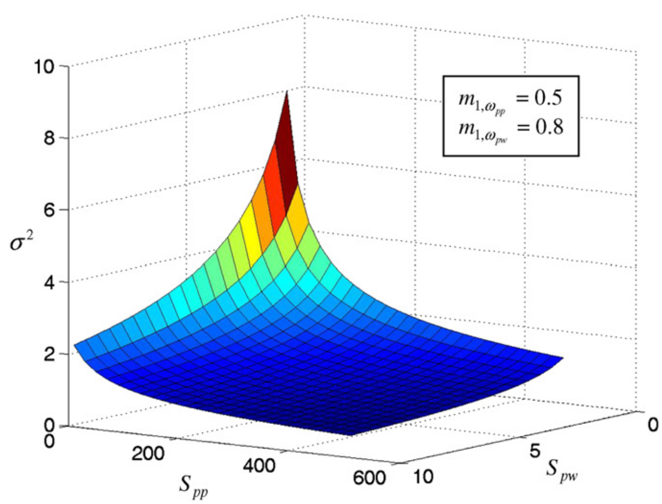

Fig. 7. The variance of temperature of the particle population as a function of frequencies of particle–particle and particle–wall collisions.

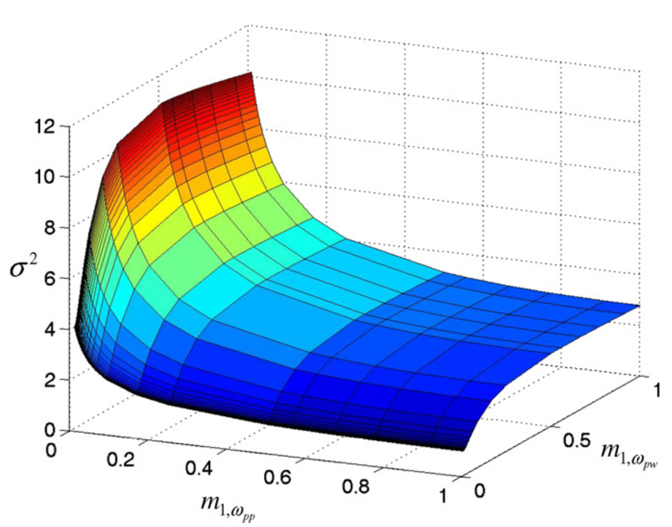

Fig. 8. The variance of temperature of the particle population as a function of the mean values of random parameters of collisional particle–particle and particle–wall heat transfers.

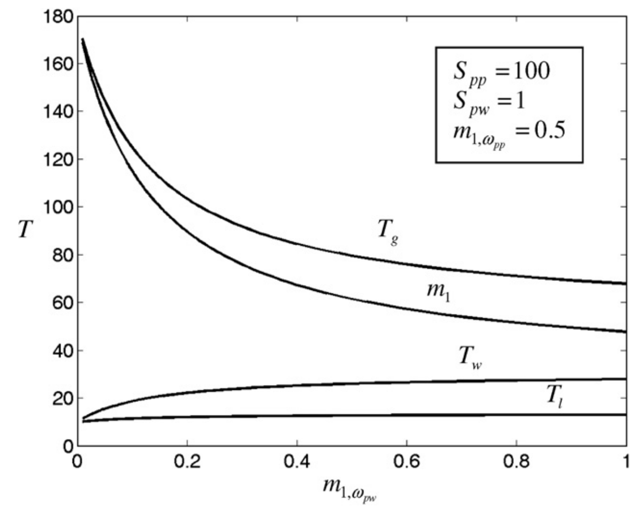

Fig. 9. Variation of steady state temperatures of the system as a function of the collisional particle–wall heat transfer.

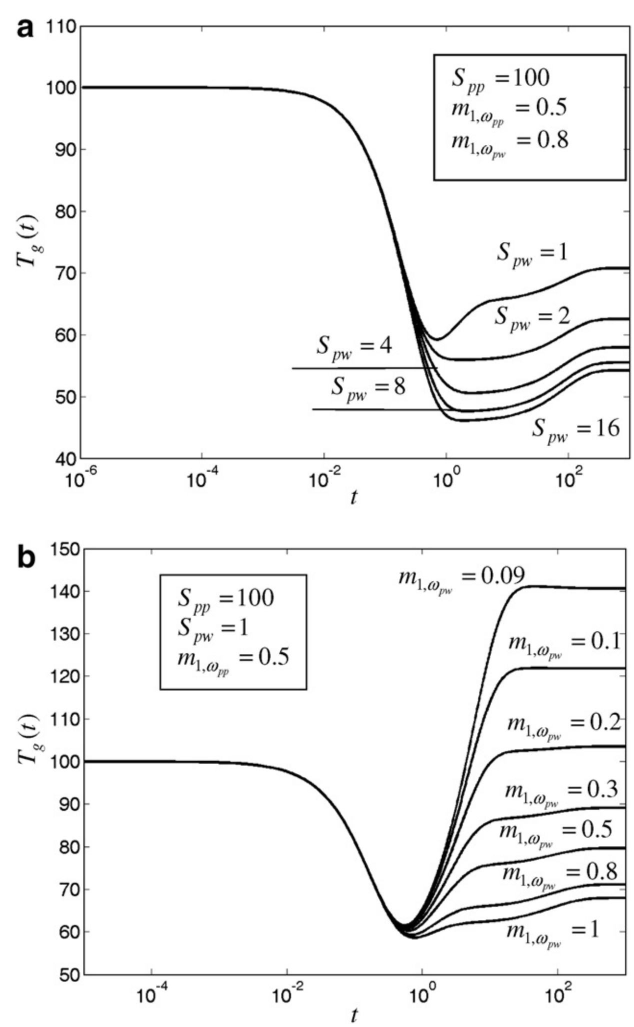

Fig. 10. Transients of the gas temperature as a function of (a) parameter S_{pw} and (b) parameter $m_{1,\omega_{pw}}$.

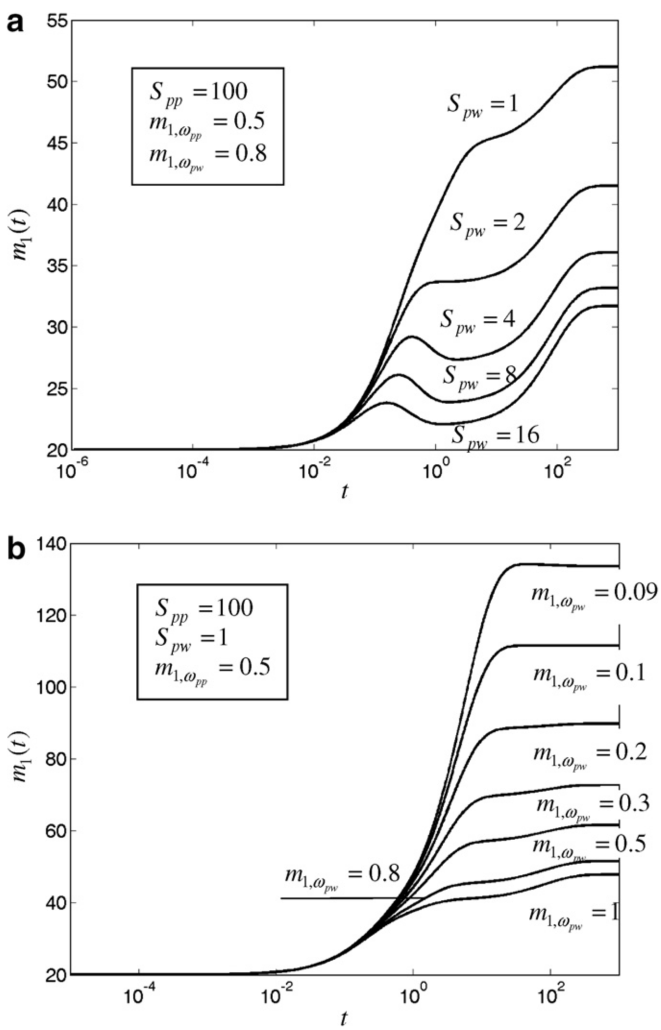

Fig. 11. Transients of the mean temperature of particle population as a function of (a) parameter S_{pw} and (b) parameter $m_{1,\omega_{\mathrm{pw}}}$.

transfers significantly as it is shown in Fig. 7 for different frequencies of collisions keeping the heat transfer coefficients constant. Similar effects are seen in Fig. 8 where the dependence of the variance of temperature of particle population is shown as a function of the mean values of random parameters ω_{pp} and ω_{pw}, characterising the intensities of heat transfer processes occurring during collisions. In these simulation runs the variances of random parameters ω_{pp} and ω_{pw} were zero.

Figs. 7 and 8 illustrate well that the collisional particle–particle and particle–wall heat transfers contribute to homogenisation of the temperature of particle population to a large extent. This homogenisation effect appears to be especially important when such nonlinear temperature-dependent processes with strong thermal effects, as catalytic reactions or drying of particles take place on the particles themselves. At the same time, collisional particle–particle heat transfers no affect the mean temperature of particle population at all. In fact, the collisional interparticle heat transfer no influences the temperatures in the processing system even in transient states as it can be concluded directly from the model equations (43)–(45), (45)–(48).

The collisional particle–wall heat transfer affects all temperatures of the system significantly as it is illustrated by the graphs presented in Fig. 9 for different mean values of parameter ω_{pw}. In this case, the wall absorbs an increased amount of heat so that division of the heat between the population of particles and the wall occurs for the good of wall.

Transients of the gas temperature and the mean temperature of particle population as a function of parameters S_{pw} and $m_{1,\omega_{\mathrm{pw}}}$ are presented in Figs. 10 and 11, showing that the intensity of collisional particle–wall heat transfer affects also the dynamic properties of the system. The semi-logarithmic plots in Figs. 10 and 11 emphasize well that under some conditions the transient processes of both the gas temperature and the mean value of temperature of particle population exhibit overshoots and even damped oscillations that should be taken into account in developing control systems for jacketed gas–solid fluidized beds.

7. Conclusions

A population balance model was developed for heat transfer processes in gas–solid systems with intensive motion of particles by means of which the distribution of temperature of the particle population can be described in detail. The population balance equation, characterising the thermal behaviour of the particulate phase, was derived as a special case of the population balance equation derived for modelling interactive populations of disperse systems of chemical engineering. Collisional particle–particle and particle–wall heat transfers are formulated as discontinuous heat exchange processes characterised by means of random parameter models of two colliding bodies while the gas–particle, gas–wall and wall–environment heat transfers are described as continuous processes. It was shown that the wall can be treated as a second, degenerate single element population in modelling heat transfers induced by particle–wall collisions. In order to focus on developing the population balance equations for particle–particle and particle–wall collisional heat transfers, a spatially homogeneous gas–solid vessel was applied as a model system.

An infinite hierarchy of moment equations describing the time evolution of moments of particle temperature was derived from the population balance equation. This infinite set of ordinary differential equations can be closed at any order of moments so that, when continuous gas–particle, gas–wall and wall–environment heat transfers are modelled making use of linear forces, heat transfers in fluid–solid particulate systems involving particle–particle and particle–wall collisions can be described by means of the moment equation model efficiently.

The properties of the model making use of describing heat transfer processes in a gas fluidized bed with cooling jacket were investigated by numerical experiments using the second order moment equation model. It was shown that increasing gas velocity increases also the inhomogeneities of the temperature distribution of particles while collisional particle–particle and particle–wall heat transfers contribute to homogenisation of the temperature of particle population to a large extent. The collisional particle–particle heat transfer no affects the mean temperature of particle population and, in fact, no influences any of temperatures in the system whilst the particle–wall collisional heat transfer exhibits significant influence not only on the steady state temperatures but on the transient processes of the system as well.

The population balance model was developed under the assumption of a spatially homogeneous gas–solid system but it allows describing spatial distributions of gas and particle temperatures in processing units by means of compartmental models formed as networks of perfectly mixed gas–solid cells as it was presented by Süle et al.[19] in modelling fluid–solid heat exchangers.

References

[1] E.U. Schlünder, Heat transfer to packed and stirred beds from the surface of immersed bodies, Chem. Eng. Proc. 18 (1984) 31–53.
[2] H. Martin, Heat transfer between gas fluidized bed of solid particles and the surfaces of immersed heat transfer exchanger elements, Chem. Eng. Proc. 18 (1984) 199–223.
[3] J. Sun, M.M. Chen, A theoretical analysis of heat transfer due to particle impact, Int. J. Heat Mass Transfer 31 (1988) 969–975.
[4] J. Vanderschuren, C. Delvosalle, Particle-to-particle heat transfer in fluidized bed drying, Chem. Eng. Sci. 35 (8) (1980) 1741–1748.
[5] C. Delvosalle, J. Vanderschuren, Gas-to-particle and particle-to-particle heat transfer in fluidized beds of large particles, Chem. Eng. Sci. 40 (5) (1985) 769–779.
[6] O. Molerus, Heat transfer in moving beds with a stagnant interstitial gas, Int. J. Heat Mass Transfer 40 (1997) 4151–4159.
[7] T. Blickle, B.G. Lakatos, Cs. Mihálykó, Mathematical Models of Particulate Systems, New Results in Chemistry-89, Akadémiai Kiadó, 2001, pp. 173–348 (in Hungarian).
[8] Cs. Mihálykó, B.G. Lakatos, T. Blickle, Modelling heat transfer between solid particles, Math. Comp. Simul. 53 (2000) 403–408.
[9] J. Li, D.J. Mason, A computational investigation of transient heat transfer in pneumatic transport of granular particles, Powder Technol. 112 (2002) 273–282.
[10] D. Lathouwers, J. Bellan, Modeling of dense gas–solid reactive mixtures applied to biomass pyrolysis in a fluidized bed, Int. J. Multiphase Flow 27 (2001) 2155–2187.
[11] Z. Mansoori, M. Saffar-Avval, H. Basirat-Tabrizi, G. Ahmadi, S. Lain, Thermo-mechanical modeling of turbulent heat transfer in gas–solid flows including particle collisions, Int. J. Heat Fluid Flow Transfer 23 (2002) 792–806.
[12] J. Burgschweiger, E. Tsotas, Experimental investigation and modelling of continuous fluidized drying under steady-state and dynamic conditions, Chem. Eng. Sci. 57 (2002) 5021–5038.
[13] H. Zhou, G. Flamant, D. Gauthier, DEM-LES simulation of coal combustion in a bubbling fluidized bed. Part II: Coal combustion at the particulate level, Chem. Eng. Sci. 59 (2004) 4205–4215.
[14] Cs. Mihálykó, B.G. Lakatos, A. Matejdesz, T. Blickle, Population balance model for particle-to-particle heat transfer in gas–solid systems, Int. J. Heat Mass Transfer 47 (2004) 1325–1334.
[15] Z. Mansoori, M. Saffar-Avval, H. Basirat-Tabrizi, B. Dabir, G. Ahmadi, Inter-particle heat transfer in a riser of gas–solid turbulent flows, Powder Technol. 159 (2005) 35–45.
[16] V. Chagras, B. Osterlé, P. Boulet, On heat transfer in gas–solid pipe flows: Effects of collision induced alterations on the flow dynamics, Int. J. Heat Mass Transfer 48 (2005) 1649–1661.
[17] B.G. Lakatos, Cs. Mihálykó, T. Blickle, Modelling of interactive populations of disperse systems, in: Proc. 2nd Int. Conf. Population Balance Modelling, Valencia, 2004, pp. 72–86.
[18] B.G. Lakatos, Cs. Mihálykó, T. Blickle, Modelling of interactive populations of disperse systems, Chem. Eng. Sci. 61 (2006) 54–62.
[19] Z. Süle, Cs. Mihálykó, B.G. Lakatos, Modelling of heat transfer processes in particulate systems, in: W. Marquardt, C. Pantelides (Eds.), Proc. 16th ESCAPE and 9th ISPSE. Comp-Aided Chem. Eng, vol. 21A, Elsevier, Amsterdam, 2006, pp. 589–594.
[20] M. Sommerfeld, Validation of a stochastic Lagrangian modelling approach for inter-particle collisions in homogeneous isotropic turbulence, Int. J. Multiphase Flow 27 (2001) 1829–1858.
[21] M. Sommerfeld, Kinetic simulations for analysing the wall collision process of non-spherical particles, in: Proc. ASME FEDSM'02, 2002, pp. 1–9.
[22] M. Hamidipour, N. Mostoufi, R. Sotudeh-Gharebagh, J. Chaouki, Monitoring the particle–wall contact in a gas fluidized bed by RPT, Powder Technol. 153 (2005) 119–126.
[23] M. Hamidipour, N. Mostoufi, R. Sotudeh-Gharebagh, J. Chaouki, Experimental investigation of particle contact time at the wall of gas fluidized beds, Chem. Eng. Sci. 60 (2005) 4349–4357.
[24] D. Gidaspow, Multiphase Flow and Fluidization, Academic Press, Boston, 1994.
[25] C.Y. Wen, Y.H. Yu, A generalized method for predicting minimum fluidization velocity, AIChE J. 12 (1966) 610–618.
[26] H. Kölbel, E. Borchers, J. Martins, Wärmeübergang in Blasensäulen III. Messungen an gasdurchströmten Suspensionen, Chem.-Ing.-Techn. 32 (1960) 84–88.
[27] A.P. Baskakov, V.M. Suprun, The determination of the convective component of the coefficient of heat transfer to a gas in a fluidized bed, Int. Chem. Eng. 12 (1972) 53–62.
[28] J.F. Richardson, P. Ayers, Heat transfer between particles and a gas in a fluidised bed, Trans. Inst. Chem. Eng. 37 (1959) 314–321.